104 MHz rate single-shot recording with subpicosecond resolution using temporal imaging

Vincent J. Hernandez,[1] Corey V. Bennett,[1,*] Bryan D. Moran,[1] Alexander D. Drobshoff,[1] Derek Chang,[1,2] Carsten Langrock,[2] Martin M. Fejer,[2] and Morten Ibsen[3]

[1]*Lawrence Livermore National Laboratory, P.O. Box 808, Livermore, CA 94550, USA*
[2]*Edward L. Ginzton Laboratory, Stanford University, Stanford, CA 94305, USA*
[3]*Optoelectronics Research Centre, University of Southampton, Highfield, Southampton, Hampshire. SO17 1BJ, UK*
[*]*cvbennett@llnl.gov*

Abstract: We demonstrate temporal imaging for the measurement and characterization of optical arbitrary waveforms and events. The system measures single-shot 200 ps frames at a rate of 104 MHz, where each frame is time magnified by a factor of –42.4x. Impulse response tests show that the system enables 783 fs resolution when placed at the front end of a 20 GHz oscilloscope. Modulated pulse trains characterize the system's impulse response, jitter, and frame-to-frame variation.

OCIS codes: (320.7100) Ultrafast measurements; (190.4410) Nonlinear optics, parametric processes.

References and links

1. G. H. Miller, E. I. Moses, and C. R. Wuest, "The National Ignition Facility: enabling fusion ignition for the 21st century," Nucl. Fusion **44**(12), S228–S238 (2004).
2. S. P. Vernon, M. E. Lowry, K. L. Baker, C. V. Bennett, J. R. Celeste, C. Cerjan, S. Haynes, V. J. Hernandez, W. W. Hsing, G. A. Lacaille, R. A. London, B. Moran, A. S. von Wittenau, P. T. Steele, and R. E. Stewart, "X-ray bang-time and fusion reaction history at picosecond resolution using RadOptic detection," Rev. Sci. Instrum. **83**(10), 10D307 (2012).
3. L. Bonnet, T. Pierzchala, K. Piotrzkowski, and P. Rodeghiero, "GASTOF: ultra-fast TOF forward detector for exclusive processes at the LHC," Acta Phys. Pol. B **38**, 477–482 (2007).
4. S. T. Cundiff and A. M. Weiner, "Optical arbitrary waveform generation," Nat. Photonics **4**(11), 760–766 (2010).
5. N. K. Fontaine, R. P. Scott, and S. J. B. Yoo, "Dynamic optical arbitrary waveform generation and detection in InP photonic integrated circuits for Tb/s optical communications," Opt. Commun. **284**(15), 3693–3705 (2011).
6. P. J. Delfyett, I. Ozdur, N. Hoghooghi, M. Akbulut, J. Davila-Rodriguez, and S. Bhooplapur, "Advanced ultrafast technologies based on optical frequency combs," IEEE J. Sel. Top. Quantum Electron. **18**(1), 258–274 (2012).
7. R. Trebino, *Frequency-resolved optical gating: the measurement of ultrashort laser pulses* (Kluwer Academic, Boston, Mass., 2000).
8. C. Iaconis and I. A. Walmsley, "Self-referencing spectral interferometry for measuring ultrashort optical pulses," IEEE J. Quantum Electron. **35**(4), 501–509 (1999).
9. P. Tournois, J. L. Vernet, and G. Bienvenu, "Sur l'analogie optique de certains montages électroniques: Formation d'images temporelles de signaux électriques," C. R. Acad. Sci. **267**, 375–378 (1968).
10. W. J. Caputi, "Stretch: a time-transformation technique," IEEE Trans. Aerosp. Electron. Syst. **AES-7**(2), 269–278 (1971).
11. B. H. Kolner, "Space-time duality and the theory of temporal imaging," IEEE J. Quantum Electron. **30**(8), 1951–1963 (1994).
12. C. V. Bennett and B. H. Kolner, "Principles of parametric temporal imaging - part I: system configurations," IEEE J. Quantum Electron. **36**(4), 430–437 (2000).
13. C. V. Bennett and B. H. Kolner, "Principles of parametric temporal imaging - part II: system performance," IEEE J. Quantum Electron. **36**(6), 649–655 (2000).
14. C. V. Bennett, "Ultrafast chirped optical waveform recording using referenced heterodyning and a time microscope," U.S. Patent No. 7,738,111.
15. C. V. Bennett and B. H. Kolner, "Upconversion time microscope demonstrating 103x magnification of femtosecond waveforms," Opt. Lett. **24**(11), 783–785 (1999).

#179012 - $15.00 USD Received 31 Oct 2012; revised 7 Dec 2012; accepted 10 Dec 2012; published 3 Jan 2013

16. C. V. Bennett, B. D. Moran, C. Langrock, M. M. Fejer, and M. Ibsen, "Guided-wave temporal imaging based ultrafast recorders," in *Conf. on Lasers and Electro-Optics/Quantum Electronics and Laser Science Conf. and Photonic Applications Systems Tech. (CLEO/QELS and PhAST)*, (OSA, 2007), paper CFF1.
17. C. V. Bennett, B. D. Moran, C. Langrock, M. M. Fejer, and M. Ibsen, "640 GHz real-time recording using temporal imaging," in *Conf. on Lasers and Electro-Optics/Quantum Electronics and Laser Science Conf. and Photonic Applications Systems Tech. (CLEO/QELS and PhAST)*, (OSA, 2008), paper CTuA6.
18. R. Salem, M. A. Foster, A. C. Turner, D. F. Geraghty, M. Lipson, and A. L. Gaeta, "Optical time lens based on four-wave mixing on a silicon chip," Opt. Lett. **33**(10), 1047–1049 (2008).
19. R. Salem, M. A. Foster, A. C. Turner-Foster, D. F. Geraghty, M. Lipson, and A. L. Gaeta, "High-speed optical sampling using a silicon-chip temporal magnifier," Opt. Express **17**(6), 4324–4329 (2009).
20. D. H. Broaddus, M. A. Foster, O. Kuzucu, A. C. Turner-Foster, K. W. Koch, M. Lipson, and A. L. Gaeta, "Temporal-imaging system with simple external-clock triggering," Opt. Express **18**(13), 14262–14269 (2010).
21. M. T. Kauffman, W. C. Banyai, A. A. Godil, and D. M. Bloom, "Time-to-frequency converter for measuring picosecond optical pulses," Appl. Phys. Lett. **64**(3), 270–272 (1994).
22. M. A. Foster, R. Salem, D. F. Geraghty, A. C. Turner-Foster, M. Lipson, and A. L. Gaeta, "Silicon-chip-based ultrafast optical oscilloscope," Nature **456**(7218), 81–84 (2008).
23. J. Azaña, L. R. Chen, M. A. Muriel, and P. W. E. Smith, "Experimental demonstration of real-time Fourier transformation using linearly chirped fibre Bragg gratings," Electron. Lett. **35**(25), 2223–2224 (1999).
24. Y. Han and B. Jalali, "Photonic time-stretched analog-to-digital converter: fundamental concepts and practical considerations," J. Lightwave Technol. **21**(12), 3085–3103 (2003).
25. M. H. Asghari, Y. Park, and J. Azaña, "Complex-field measurement of ultrafast dynamic optical waveforms based on real-time spectral interferometry," Opt. Express **18**(16), 16526–16538 (2010).
26. R. P. Scott, N. K. Fontaine, D. J. Geisler, and S. J. B. Yoo, "Frequency-to-time-assisted interferometry for full-field optical waveform measurements with picosecond resolution and microsecond record lengths," IEEE Photon. J. **4**(3), 748–758 (2012).
27. M. H. Asghari and B. Jalali, "Stereopsis-inspired time-stretched amplified real-time spectrometer (STARS)," IEEE Photon. J. **4**(5), 1693–1701 (2012).
28. D. H. Broaddus, M. A. Foster, O. Kuzucu, K. W. Koch, and A. L. Gaeta, "Ultrafast, single-shot phase and amplitude measurement via a temporal imaging approach," in *Conf. on Lasers and Electro-Optics/Quantum Electronics and Laser Science Conf. (CLEO/QELS)*, (OSA, 2010), paper CMK6.
29. R. P. Scott, N. K. Fontaine, J. P. Heritage, B. H. Kolner, and S. J. B. Yoo, "3.5-THz wide, 175 mode optical comb source," in *Optical Fiber Communication and the National Fiber Optic Engineers Conf. (OFC/NFOEC)*, (OSA, 2007), paper OWJ3.
30. S. D. Yang, A. M. Weiner, K. R. Parameswaran, and M. M. Fejer, "400-photon-per-pulse ultrashort pulse autocorrelation measurement with aperiodically poled lithium niobate waveguides at 1.55 microm," Opt. Lett. **29**(17), 2070–2072 (2004).
31. M. Durkin, M. Ibsen, M. J. Cole, and R. I. Laming, "1m long continuously-written fibre Bragg gratings for combined second- and third-order dispersion compensation," Electron. Lett. **33**(22), 1891–1893 (1997).

1. Introduction

Rapid advances in engineering, science, and physics is driving the need for measurement techniques that capture signals spanning ever-shortening time scales. Measurements discerning subpicosecond detail will be required to characterize and fully understand a wide variety of phenomena, such as optically-detectable fusion burn on the National Ignition Facility (NIF) [1, 2], particle counting and time-of-flight measurement on the Large Hadron Collider (LHC) [3], and optical arbitrary waveform generation (OAWG) for advanced LIDAR and laser communication [4–6]. These varied applications require a technique that employs real-time data capture, long record lengths, and single shot measurement. For OAWG in particular, frame rates exceeding 100 MHz are desired. Well-established technologies such as oscilloscopes and streak cameras have extended recording lengths and capture real-time single-shot data; however, oscilloscopes are bandwidth limited while streak cameras have limited frame rates. Techniques specialized for ultrafast signals, such as frequency resolved optical gating (FROG) [7] and spectral phase interferometry for direct electric-field reconstruction (SPIDER) [8] are limited in time-bandwidth product. Additionally, they often require slow scanning, repetitive signals, or considerable post-processing.

Temporal imaging [9–11] is a promising alternative to these approaches, bridging the gap between real-time, extended-length recording instruments and the ultrafast techniques. This scheme manipulates signals in the time domain through careful application of both group

#179012 - $15.00 USD Received 31 Oct 2012; revised 7 Dec 2012; accepted 10 Dec 2012; published 3 Jan 2013

delay dispersion (GDD) and quadratic temporal phase modulation (linear frequency chirp). The physics of the latter are analogous to the application of spatial phase modulation onto a beam of light by a conventional lens. Thus, just as one can image and magnify an object in space using a lens, one can *temporally* image and magnify a waveform using a "time lens." The time lens can then be applied to the front end of a recording device, such that detail that previously exceeded the bandwidth capabilities of the recording device become discernable. In the generalized temporal imaging process, a signal is propagated through an input GDD ϕ_1'', imparted with a linear chirp $d\omega/d\tau$ through the time lens, and then propagated through an output GDD ϕ_2''. Techniques for implementing the time lens vary and dictate the corresponding media used for the GDD. Parametric systems employ nonlinear optical processes, which imparts quadratic phase by mixing the signal with a linearly chirped pump pulse [12–14]. Demonstrated parametric temporal imaging systems have thus far have relied on time lenses using either sum-frequency generation (SFG) [13, 15–17] or four-wave mixing (FWM) [18–20]. Temporal imaging should not be confused with time-to-frequency conversion, where the spectral output of the time lens corresponds to a magnified temporal profile that can be captured directly on a spectrometer [15, 21, 22]. Such systems have limited frame rates due to the speed of the spectrometer camera (currently about 100 kHz).

Temporal imaging systems and other ultrafast techniques may be characterized by their equivalent continuous time bandwidth (ECT-BW), which we define as frame-length-to-resolution ratio times the frame rate, or the repetition rate times the number of resolvable points per frame. The repetition rate times the frame length converges to one for continuous measurements; therefore, it can also be viewed as the fraction of continuous time divided by the system resolution. A true continuously recording picosecond resolution system would then have an ECT-BW = 1 THz. For SFG-based temporal imaging, the highest demonstrated ECT-BW = 100 ps / 900 fs x 155 MHz = 17.2 GHz [17]; for FWM-based temporal imaging, ECT-BW = 200 ps / 1.5 ps x 40 MHz = 5.9 GHz [20]. Other ultrafast techniques have lately been demonstrated incorporating optical time stretching, where optical dispersion is used to slow down ultrafast-encoded signals [23, 24]. In [25], real time spectral interferometry is combined with time stretching to achieve 350 ps record lengths with 400 fs rise-time-based resolution at 17 MHz, or an ECT-BW = 14.9 GHz. An extension of this work employing four-quadrature coherent detection has demonstrated 700 ps record length with ~786 fs resolution (based on 560 GHz and a Gaussian response) at 40 MHz [26], or ECT-BW = ~35.7 GHz. Recently, a stereopsis-inspired time-stretched amplified real-time spectrometer (STARS) [27] has been demonstrated, employing a stereopsis reconstruction algorithm to recover self-referenced time-stretched signals at 25 MHz. This work alludes to an ECT-BW as high as 875 GHz, based on separate experiments that temporally measure ~1 ps input pulses over 250 ps and the group delay verses frequency of a pulse dispersed across 35 ns. However, the work does not explicitly claim a resolution, nor show a temporal amplitude measurement across 35 ns simultaneously having ultrafast detail. All of these optical time stretch-assisted techniques demonstrate phase and amplitude recovery of the signal, a feature likewise available using FROG and SPIDER. The aforementioned temporal imaging demonstrations, including the one discussed here, strictly characterize the magnitude of the signal. However, it should be noted that temporal imaging is capable of phase and amplitude recovery [14] and this has been demonstrated in a non-repetitive implementation [28].

In this paper, we investigate a parametric temporal imaging system based on SFG. Under this nonlinear process, a waveform is temporally imaged when the following condition is met [12]:

$$\frac{1}{\phi_1''}+\frac{1}{\phi_2''}=\frac{1}{\phi_f''} \tag{1}$$

#179012 - $15.00 USD Received 31 Oct 2012; revised 7 Dec 2012; accepted 10 Dec 2012; published 3 Jan 2013

where $\phi_f'' = -(d\omega/d\tau)^{-1}$ is the focal dispersion, the negative inverse of the imparted linear chirp. Equation (1) takes on a similar form to the well-known thin lens equation in diffractive optics. The ratio $M = -\phi_2''/\phi_1''$ describes a magnification of the waveform in time. Early SFG temporal imaging systems demonstrated 103x magnification and 200 fs resolution, but had limited frame length and poor signal-to-noise ratio that mandated repetitive averaging [13, 15]. More recent systems achieved −30x time magnification and true single-shot, high repetition rate recording within 100 ps frames [16, 17]. This paper presents a –42.4x magnification temporal imaging system designed for subpicosecond resolution, a frame length of 200 ps, and the highest possible repetition rate. When used as a front end to an optical receiver and 20 GHz real-time scope, 783 fs resolution is achieved. For this demonstration, we show single-shot recordings of pulses modulated with gigabit-rate data at 104.2 Mframes/s. The recordings show that the temporal imaging system is capable of capturing data streams of up to 1 Tb/s. The demonstrated ECT-BW of the system is 26.6 GHz, an improvement over the previous temporal imaging systems and comparable to the performance of systems leveraging optical time stretching (when ECT-BW can clearly be determined).

2. System description

Figure 1(a) shows the set-up of the temporal imaging system, divided into three main subsystems: input dispersion, time lens, and output dispersion. Each component is discussed in further detail below. Throughout the set-up, erbium-doped fiber optical amplifiers (OAs) are used to overcome system loss and optimize the output. Although not shown, each OA is followed by a filter used to remove any out-of-band amplified spontaneous emission. Polarization controllers (PCs) are also used throughout the system in order to optimize the outputs of polarization-sensitive elements.

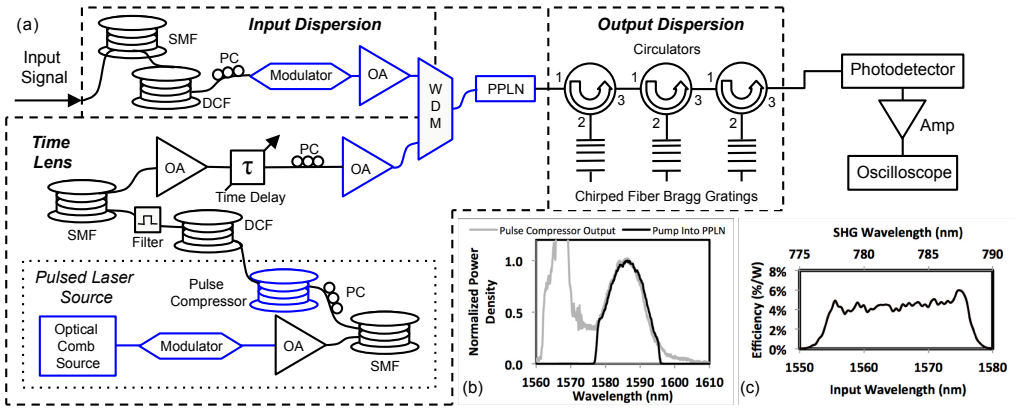

Fig. 1. (a) A-PPLN-based temporal imaging system with (b) pump spectrum and (c) A-PPLN waveguide SHG transfer function.

2.1 Input dispersion

The input dispersion applies input GDD onto incoming signals. It consists mainly of spans of single mode fiber (SMF-28) and dispersion compensating fiber (DCF), applying a total GDD of $\Phi_1'' = -22.2$ ps^2 for input signals at 1550 nm. The ratio of SMF to DCF fiber lengths minimize the combined dispersion slope, yielding a third order dispersion of $\Phi_1''' = -0.0222$ ps^3. The Mach-Zehnder modulator passes through only the portion of the signal that coincides with the pump, as aligned with a time delay in the time lens. In this way, the OA gain amplifies only the necessary portion of the signal and avoids gain saturation.

#179012 - $15.00 USD Received 31 Oct 2012; revised 7 Dec 2012; accepted 10 Dec 2012; published 3 Jan 2013

2.2 Time lens

The time lens imparts the dispersed input with chirp via nonlinear mixing (SFG) with a chirped pump. The pump originates from a pulsed laser source based on an optical comb, similar in design to [29]. In this case, the optical comb is centered at 1568 nm and has a 10 GHz repetition rate. A modulator pulse picks it down to 104.2 MHz, and then it is compressed and spectrally shifted into a near transform-limited pulse. The final pulsed laser source output is thus an unchirped pulse with 12.5 nm full width half max (FWHM) bandwidth centered near 1585 nm (Fig. 1(b)). The pulse acquires chirp by propagating through focal dispersion consisting of DCF and SMF, for a total GDD of $\Phi_f'' = -21.5$ ps^2. Again, the DCF and SMF combine to minimize the dispersion slope, yielding a third order dispersion of $\Phi_f''' = -0.0570$ ps^3. The dispersion itself widens the pump to 200 ps FWHM, the field of view of the system. The typical final pump spectrum is shown in Fig. 1(b), where filtering, erbium doped fiber optical amplifier (OA) gain, and polarization dependence cause the pump to deviate from the initial soliton. This pump is combined with the dispersed input via a wavelength division multiplexer (WDM). An aperiodically poled $LiNbO_3$ (A-PPLN) waveguide [30] is then used as the nonlinear element to impart the pump's chirp onto the signal. Figure 1(c) shows the measured second harmonic generation (SHG) produced by the fiber-coupled A-PPLN in response to a tunable laser, revealing that the A-PPLN has nearly 20 nm of bandwidth and greater than 4%/W efficiency. The calculated GVD mismatch between the pump and signal across this 45 mm device is 0.006 radian, which is considered negligible [13]. The SFG profile of the A-PPLN is thus considered four times greater than the SHG profile given. The pump entering the A-PPLN waveguide has a peak power of approximately 1.2 W, or energy of 530 pJ/pulse. The input and pump produce a sum frequency mixing product at 785 nm.

2.3 Output dispersion and detection

The output dispersion consists of a cascade of three chirped fiber Bragg gratings (FBGs) [31] that have a combined output GDD and third order dispersion of $\Phi_2'' = -941$ ps^2 and $\Phi_2''' = 1.85$ ps^3. FBGs are used in lieu of fibers, as fibers with enough dispersion and reasonable loss are not readily available at 785 nm. Despite this, the loss through the output dispersion turned out substantial at 19.3 dB. The system of all components yield a temporal imaging system with $M = -42.4$ by design. The final temporally imaged output is received on a 30 GHz optical photodetector followed by a 30 GHz electrical amplifier that overcomes the losses in the output dispersion. This is measured on a 20 GHz, 50 GSa/s real-time oscilloscope (Tektronix DSA72004). The receiver impulse response, which accounts for the receiver, amplifier, and subsequent oscilloscope electronics, is measured to be 31.6 ps FWHM.

3. System results and discussion

The system magnification is verified using a subpicosecond 2.5 GHz pulse train as an input signal, where a calibrated optical delay line controls the relative pulse position. Precise adjustments to the pulse position can then be observed as a magnified time shift at the system output. Figure 2(a) shows the observed output shift when the pulse is shifted a total of 192 ps at the input, covering most of the system field of view. A linear interpolation of the data reveals an average magnification of $M = -42.4$, in line with the design magnification. Figure 2(b) compares the width of the pulses in and out of the system, showing an input pulse width of 506 fs, measured using SHG FROG. The plotted output is the overlap of 208 pulses captured single-shot on the oscilloscope after temporal imaging, showing an average pulse width of 39.9 ps on the magnified output time scale, or 941 fs before magnification. With the input and output pulse widths known, we calculate a system impulse response (or resolution) of 793 fs, assuming the convolution of Gaussian pulses. This is in good agreement with the theoretical system response of 783 fs, which is similarly obtained by convolving the ideal

#179012 - $15.00 USD Received 31 Oct 2012; revised 7 Dec 2012; accepted 10 Dec 2012; published 3 Jan 2013

optical system resolution limit (240 fs, as established by the pump) with the scaled receiver impulse response (31.6 ps / 42.4 = 745 fs). The impulse measured at the output of the FBG had approximately 130 µW of peak power and 130 fJ of pulse energy, versus 78 mW peak power and 1.1 pJ/pulse into the temporal imaging system.

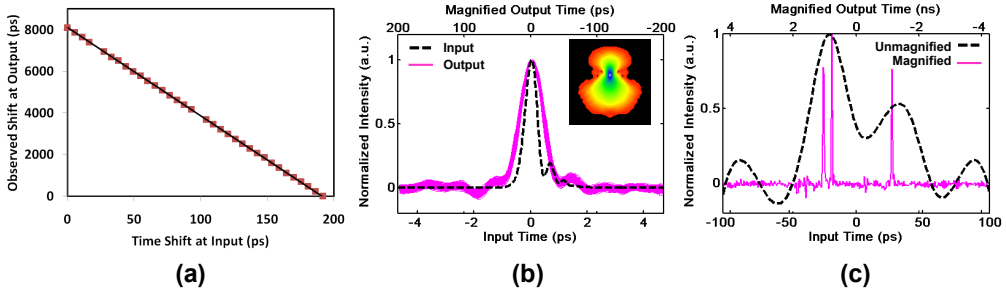

Fig. 2. Characterization of temporal imaging system: (a) observed time shifts at the output in response to adjustments made at the input, revealing a time magnification of $M = -42.4$; (b) system response to a 506 fs impulse, as measured with inset SHG FROG; (c) measurement of a three pulse packet on a 20 GHz oscilloscope without temporal imaging (unmagnified) and with temporal imaging (magnified).

Magnification and resolution improvement is further demonstrated by recording a three-pulse test packet. The packet is generated by modulating (on-off-keying) the 2.5 GHz pulse train with a pseudorandom bit sequence at 2.5 Gb/s. This is then split it into three paths with different delays and recombined. The relative delay between each path consists of several periods, so that each pulse within a packet experiences a different modulation. The second and third pulses are respectively spaced 6.1 ps and 51.4 ps away from the first pulse. Although using a lower rate modulator, the resulting pattern is similar to a 163 Gb/s data stream based on the 6.1 ps bit period. One could even consider the pattern to be a ~Tb/s data stream considering that the pulses themselves are subpicosecond. A 20 GHz oscilloscope capture of one of these packets (with all three pulses present) is shown in Fig. 2(c), employing sin(x)/x interpolation. Without temporal imaging, the oscilloscope's bandwidth limit causes the first and second pulses to appear as a single peak. In contrast, the output after magnification clearly resolves all three pulses on the magnified output time scale.

Figure 3 compares multiple frames of pulse packets before and after temporal imaging. A real-time 57.6 ns recording of the three pulse packets before temporal imaging are shown in Fig. 3(a). The temporal imaging system magnifies six packets within this record at 104 Mframes/s. The frames are shown close up in Fig. 3(b) using non-interpolated and unmagnified scope data at 50 GSa/s, where it is difficult to determine the data modulation applied to the pulses, which are indicated. Unmagnified, only 10 samples from the scope are contained within the 200 ps frames. The equivalent frames after temporal imaging are shown in Fig. 3(c), where the frames are now expanded to 8.55 ns each. The data modulation applied to each pulse becomes clearly discernable, as each frame now contains ~426 samples. With temporal imaging, the scope's equivalent bandwidth and sampling rate are 848 GHz and 2.1 Tsample/s, as referred to the input of the system. The six highlighted frames are part of a 2 µs single-shot recording containing 206 frames in Fig. 3(d).

#179012 - $15.00 USD Received 31 Oct 2012; revised 7 Dec 2012; accepted 10 Dec 2012; published 3 Jan 2013

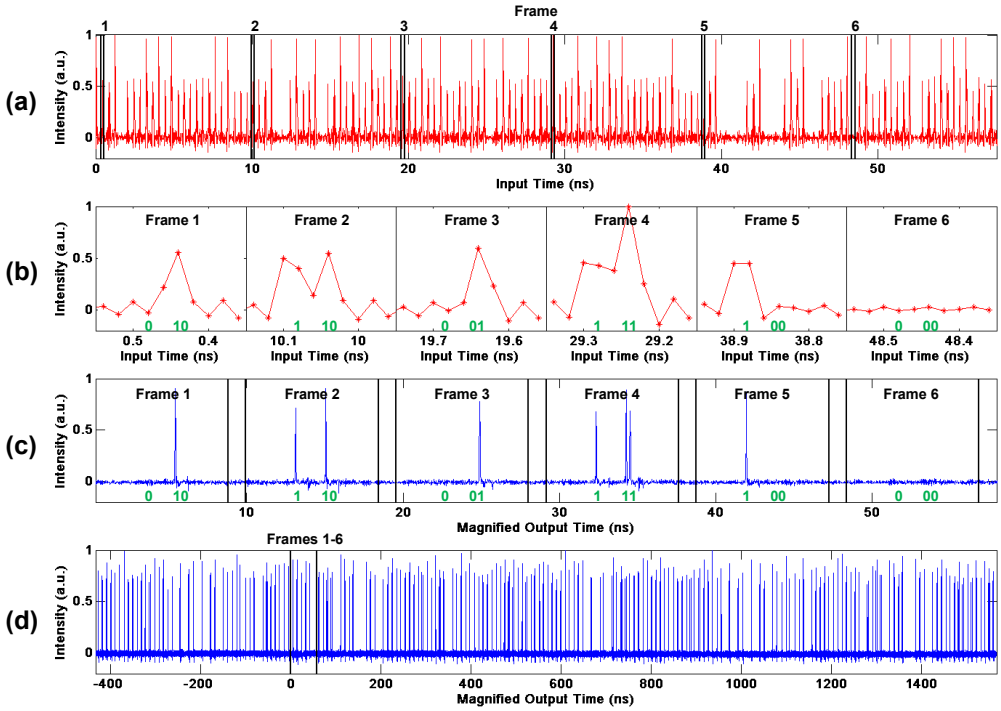

Fig. 3. Comparison of pulse packets containing data-modulated pulses before and after temporal imaging as measured from a 20 GHz real-time scope: (a) non-magnified input with (b) close-up of individual frames versus (c) close-up of time magnified output frames from (d) a single-shot 2 μs recording containing 206 total frames and resolving the individual subpicosecond pulses. The modulated data bit within the frames is indicated at the bottom of (b) and (c).

The system jitter is analyzed by overlapping the 206 frames in the 2 μs record and zooming in on each pulse, as shown in Figs. 4(a)-4(c). For this entire record, the scaled rms jitter for the first, second, and third pulses are respectively 240 fs, 180 fs, and 270 fs between frames that are 9.6 ns apart. Some of this jitter may be arising from the signal source itself, a harmonically mode-locked fiber laser. The multiple sequential pulses in these lasers are known to jitter independently [6]. Additional jitter may be caused by any differences between the signal and pump timing, which operate off of independent clocks that are synchronized through an atomic clock-generated 10 MHz reference. In particular, the 10 GHz source that drives the pump is distributed through a digital fan-out with a random jitter specification of up to 600 fs. Amplitude and pulse width variation can be determined by aligning the peaks of each pulse, thereby removing the jitter, as shown in Figs. 4 (d)-4(f). The standard deviations of the pulse peaks are found to be within 4% of their mean values: 610 mV ± 28 mV, 730 mV ± 39 mV, and 620 mV ± 46 mV. Amplitude variations between pulses within a frame can be attributed to the system aberrations that arise from the non-uniform response of the pump, A-PPLN, and fiber Bragg grating. All data being shown is a direct output from the oscilloscope and no post-processing has been applied to remove any aberration. The standard deviations of the pulse input scaled widths are found to be within 8% of their mean values: 1.17 ps ± 38 fs, 920 fs ± 35 fs, and 1.01 ps ± 38 fs.

#179012 - $15.00 USD Received 31 Oct 2012; revised 7 Dec 2012; accepted 10 Dec 2012; published 3 Jan 2013

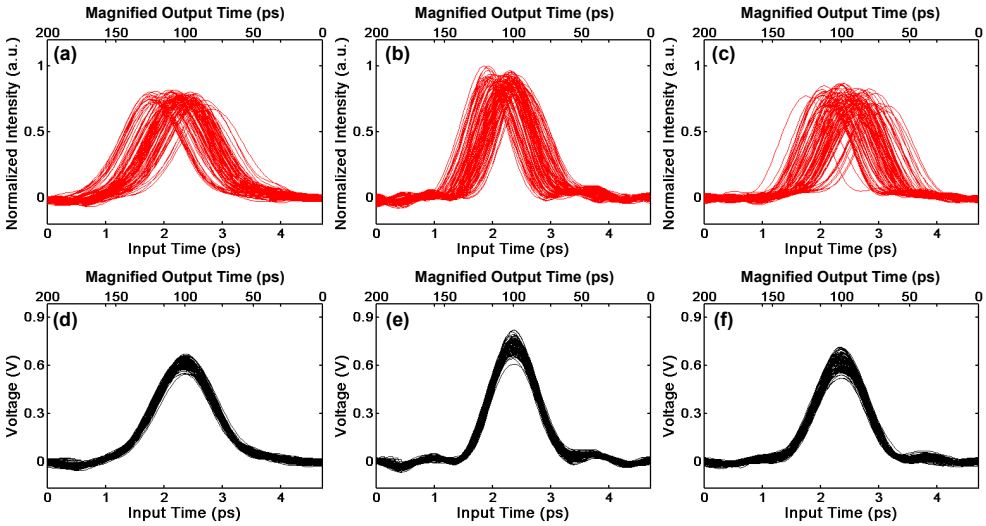

Fig. 4. Pulse-by-pulse analyses of the 206 frames in Fig. 3(d): (a-c) strict overlap of the frames, revealing frame jitter and (d-f) amplitude and width variation obtained by removing jitter.

4. Conclusion

A temporal imaging system capable of –42.4x magnification with resolution of 793 fs at 104 Mframes/s and 200 ps FWHM frame length has been demonstrated. The system resolves modulated subpicosecond pulses and a 2 μs record has been shown. The pulse separation of the record shows that the system can support data rates at 163 Gb/s, and the demonstrated resolution should accommodate data rates up to ~1 Tb/s within each frame. Finally we note that record lengths exceeding 2 μs are possible. This system is limited strictly by the memory of the digital converter, the oscilloscope. Longer records, or even continuous processing, could be performed by streaming the output to an adequate recorder or processing system.

Acknowledgments

The authors wish to thank Mario Sandoval and Tektronix for their generous equipment loan. This work performed under the auspices of the U.S. Department of Energy by Lawrence Livermore National Laboratory under Contract DE-AC52-07NA27344, and funded in part by DARPA DSO OAWG contract L-10934. LLNL-JRNL-591752

#179012 - $15.00 USD Received 31 Oct 2012; revised 7 Dec 2012; accepted 10 Dec 2012; published 3 Jan 2013